

Diffraction Dissociation of ${}^7\text{Li}$ and ${}^7\text{Be}$ Relativistic Nuclei on Proton Targets through the ${}^3\text{H}({}^3\text{He}) + {}^4\text{He}$ Channels

V. N. Fetisov*

Lebedev Physical Institute, Russian Academy of Sciences, Leninskii pr. 53, Moscow, 119991 Russia

Received December 8, 2014

Abstract—For the fragmentation of ${}^7\text{Li}$ and ${}^7\text{Be}$ relativistic nuclei (with momenta of, respectively, $P = 3 \text{ GeV}/c$ and $P = 1.6 \text{ GeV}/c$ per nucleon) on proton targets through the ${}^3\text{H}({}^3\text{He}) + {}^4\text{He}$ channels, the differential cross sections with respect to the momentum transfer Q to the fragments were calculated on the basis of the cluster version of Akhiezer–Glauber–Sitenko diffraction theory by employing the two-body cluster model for the ${}^7\text{Li}({}^3\text{H} + {}^4\text{He})$ and ${}^7\text{Be}({}^3\text{He} + {}^4\text{He})$ nuclei. These calculations, performed in the impulse approximation in the interaction of intranuclear clusters with the target nucleus, explained a strong suppression of the cross sections for reactions on protons at Q lower than $100 \text{ MeV}/c$ and higher than $350 \text{ MeV}/c$ and the observed irregularities in the behavior of the cross section for ${}^7\text{Li}$ fragmentation on complex track-emulsion nuclei. Cross-section values close to their experimental counterparts were obtained upon setting the coefficient of two-body clustering in the ${}^7\text{Li}$ and ${}^7\text{Be}$ nuclei to $k \simeq 0.7$.

DOI: 10.1134/S1063778815050051

1. INTRODUCTION

A number of experiments devoted to studying peripheral reactions involving the fragmentation of relativistic light nuclei that have momenta of several GeV/c units per nucleon and which collide with track-emulsion nuclei have been performed over the past fifteen years [1]. From the mass and charge composition of emerging fragments, it follows that not only proton emission but also the emission of deuterons, tritons, ${}^3\text{He}$ nuclei, alpha particles, and more complex nuclei may occur in such reactions. These results are usually treated, at least at a qualitative level, as manifestations of respective cluster degrees of freedom in the structure of incident nuclei. The main objective of track-emulsion experiments, in which one can study the spatial picture of events, identify charged particles, measure particle momenta and cross sections for proceeding processes, and obtain various distributions of events with respect to kinematical variables was to collect data that can be used both to study fragmentation mechanism (nuclear and Coulomb ones) and to obtain information about the structure of nuclei. It should be borne in mind, however, that a theoretical analysis of the properties of reactions involving the emission of three or more charged particles presents a very complicated problem. For this reason, multiparticle fragmentation

channels observed in track emulsions have not yet been interpreted adequately.

The situation around the application of already developed theoretical approaches to studying the structure of nuclei and fragmentation mechanisms is more favorable in those cases where the disintegration of a relativistic nucleus in a track emulsion (without the breakup of the target nucleus) leads to the formation of only two charged fragments. As examples of such reactions, one can consider the disintegration of three two-cluster nuclei ${}^6\text{Li}({}^2\text{H} + {}^4\text{He})$, ${}^7\text{Li}({}^3\text{H} + {}^4\text{He})$, and ${}^7\text{Be}({}^3\text{He} + {}^4\text{He})$ through the respective cluster channels, which are dominant in the ground states of these nuclei. A relatively large yield of such events in which the masses and charges of cluster pairs were identified was observed in nuclear track emulsions [2–4]. Track emulsions make it possible to detect all events concentrated in a very narrow cone along the direction of the beam of primary nuclei and to measure the transverse momentum of the center of mass of the final fragment pair, Q , for any polar and azimuthal emission angles of individual fragments, this being equivalent to integrating the momentum distribution for the relative motion of two clusters. As a result, one can get an idea of the distribution of all events (this is of importance in the case of a moderately small data sample, which is characteristic of the track-emulsion method) with respect to the variable Q alone and single out, in the differential cross section $d\sigma/dQ$, regions where the diffraction and Coulomb

*E-mail: ffetisov@mail.ru

reaction mechanisms are operative. In addition, this representation of the results permits comparing the theoretically predicted diffraction oscillations in the inelastic-reaction cross section with the diffraction picture observed in elastic scattering.

In [5], the results of measurements of the differential cross section $d\sigma/dQ$ for the disintegration of ${}^7\text{Li}$ nuclei (at a momentum of $P = 3 \text{ GeV}/c$ per nucleon) on track-emulsion nuclei through the ${}^3\text{H} + {}^4\text{He}$ channel were presented and were interpreted within the two-body model of the ${}^7\text{Li}$ nucleus [6, 7] and the cluster version of Akhiezer–Glauber–Sitenko diffraction theory [8–11]. One of the conclusions of that study was that the irregularities observed in the Q dependence of the cross section arise owing to the superposition of two diffraction cross sections for reactions on a mixture of light (C, N, and O) and heavy (Br and Ag) track-emulsion nuclei. Each of the masked cross sections [5, 12] has its own pronounced oscillating shape, with the first maximum being shifted (and the number of subsequent oscillations being accordingly smaller) toward the region of high values of Q for the light target nuclei, whose radii are approximately one-half as large as the radii of the heavy target nuclei. In order to discover and study the theoretically predicted features of cross-section oscillations, such as the numbers of peaks and their intensities and shifts for various values of the target mass number, one needs data on two-cluster fragmentation on individual nuclei. In track emulsions, protons are the only pure nuclear target on which one can study two-cluster fragmentation. The disintegration of ${}^7\text{Li}$ (at a momentum of $P = 3 \text{ GeV}/c$ per nucleon) and ${}^7\text{Be}$ (at a momentum of $P = 1.6 \text{ GeV}/c$ per nucleon) nuclei on proton targets in a track emulsion were recently studied in [13, 14]. The sections that follow present the elements of the formalism used here and the results obtained by calculating cross sections for two-cluster fragmentation on protons on the basis of the two-body model for the ${}^7\text{Li}$ and ${}^7\text{Be}$ nuclei and with the aid of diffraction theory. The results are compared with experimental data.

2. FORMALISM OF DIFFRACTION THEORY FOR THE TWO-CLUSTER FRAGMENTATION OF NUCLEI

Following the formalism developed in [8] and used there to derive expressions for the amplitudes and cross sections for the diffraction dissociation of a deuteron to the constituent neutron and proton, we will consider the analogous differential cross section for the fragmentation of a relativistic nucleus whose ground-state wave function $\varphi_{j_i, \mu_i}(\mathbf{r})$ has a

two-cluster form and for which $\varphi_{\mathbf{f}, \mu_s}(\mathbf{r})$ denotes the wave function for the pair of fragments in the continuous spectrum. Within this formalism, the cross section in question has the form

$$d\sigma/dQ = \frac{1}{k^2(2\pi)^3} \left\{ \frac{1}{(2j_i + 1)} \times \sum_{\mu_s, \mu_i} \int |T(\mathbf{f}, \mathbf{Q}; \mu_s, \mu_i)|^2 d\mathbf{f} d\psi_Q \right\} Q, \quad (1)$$

where k is the projectile-nucleus momentum, \mathbf{Q} is the momentum of the fragment center of mass, ψ_Q is the azimuthal angle of the vector \mathbf{Q} , and \mathbf{f} is the momentum of the relative motion of fragments. The reaction amplitude corresponding to the impulse approximation can be written in the standard form [10, 11]

$$T = \frac{k}{k_1} f_1(Q) F(\beta_1 \mathbf{Q}, \mathbf{f}) + \frac{k}{k_2} f_2(Q) F(-\beta_2 \mathbf{Q}, \mathbf{f}). \quad (2)$$

In this expression, k_1 and k_2 are the cluster momenta in the relativistic projectile nucleus ($k = k_1 + k_2$); $\beta_1 = m_2/(m_1 + m_2)$, where m_i are the cluster masses; $\beta_2 = 1 - \beta_1$; and $f_i(Q)$ are the amplitudes for the elastic scattering of individual projectile clusters on the nuclear target. These amplitudes can be expressed in terms of the integral of the product of the Bessel function $J_0(x)$ and the profile function $\omega_i(b)$ with respect to the impact parameter b as

$$f_i(Q) = ik_i \int_0^\infty J_0(Qb) \omega_i(b) b db, \quad (3)$$

$$\omega_i(\mathbf{b}) = \frac{1}{2\pi i k_i} \int \exp(-i\mathbf{q}\mathbf{b}) f_i(\mathbf{q}) d^2q.$$

The inelastic form factors

$$F(\beta_i \mathbf{Q}, \mathbf{f}) = \int \exp(i\beta_i \mathbf{Q}\mathbf{r}) \varphi_{\mathbf{f}, \mu_s}^*(\mathbf{r}) \varphi_{j_i, \mu_i}(\mathbf{r}) d\mathbf{r} \quad (4)$$

and, hence, the cross section $d\sigma/dQ^2$ vanish, in contrast to what we have in the case of elastic scattering, at $Q = 0$ by virtue of the orthogonality of the wave functions $\varphi_{\mathbf{f}, \mu_s}(\mathbf{r})$ and $\varphi_{j_i, \mu_i}(\mathbf{r})$.

Taking into account the completeness of states of the two-cluster Hamiltonian in performing integration with respect to the momentum \mathbf{f} , we can express the cross section in (1) in terms of the amplitudes $\bar{f}_i = (k/k_i) f_i(Q)$ and the radial integrals of the spherical Bessel functions $j_L(qr)$ over the bounded states R_{lj} as

$$d\sigma/dQ = \frac{2\pi}{k^2} \left(|\bar{f}_1|^2 + |\bar{f}_2|^2 \right) \quad (5)$$

$$\begin{aligned}
 &+ 2\text{Re}(\bar{f}_1 \bar{f}_2^*) I_0(Q) - 3 \sum_{l,j,L} (2l+1)(2j+1) \\
 &\times |\bar{f}_1 I_L^{lj}(\beta_1 Q) + (-1)^L \bar{f}_2 I_L^{lj}(\beta_2 Q)|^2 \\
 &\times (10l0|L0)^2 \left\{ \begin{matrix} j & l & 1/2 \\ 1 & 3/2 & L \end{matrix} \right\}^2 \Big) Q.
 \end{aligned}$$

The integrals

$$\begin{aligned}
 I_0(q) &= \int_0^\infty j_0(qr) R_i^2 r^2 dr, \\
 I_L^{lj}(q) &= \int_0^\infty j_L(qr) R_{lj} R_i r^2 dr
 \end{aligned} \quad (6)$$

are determined by the set $\{R_{i,j}\}$ of radial functions for all bounded states of the pairs of clusters (R_i is the radial function for the $P_{3/2}$ ground state), including both the states of the two-cluster Hamiltonian that are allowed by the Pauli exclusion principle and the states that are forbidden by it. We note that, in the approximation where the profile functions are equal to each other, $\omega_1(b) = \omega_2(b)$, expression (5) reduces to the analogous form presented in [5] and used there to calculate the cross sections for the two-cluster fragmentation of ${}^7\text{Li}$ nuclei on the two groups of track-emulsion nuclei [(C, N, and O) and (Br and Ag)].

The differential cross sections (5) for the fragmentation of ${}^7\text{Li}$ and ${}^7\text{Be}$ nuclei were calculated by using the diffraction amplitude for the scattering of the intranuclear clusters ${}^3\text{H}$, ${}^3\text{He}$, and ${}^4\text{He}$ on protons in the analytic form

$$\begin{aligned}
 f_i(Q) &= \frac{ik_i \sigma (1 - i\alpha)}{4\pi} \sum_{n=1}^A \frac{(-1)^{n-1}}{n} \binom{A}{n} \\
 &\times \left(\frac{\sigma (1 - i\alpha)}{2\pi(R_A^2 + 2a)} \right)^{n-1} \\
 &\times \exp \left(- \left(\frac{R_A^2 + 2a}{4n} - \frac{R_A^2}{4A} \right) Q^2 \right),
 \end{aligned} \quad (7)$$

where A is the number of nucleons in the nucleus, σ is the total cross section for nucleon–nucleon interaction, and α is the ratio of the real and imaginary parts of the amplitude for elastic scattering at zero angle. This expression for the amplitude describes fairly well the scattering of relativistic protons (at a momentum of $P_{\text{Lab}} = 1.7 \text{ GeV}/c$) on ${}^4\text{He}$ nuclei [15]. The parameters in expression (7) are related in a standard way to the nuclear density $|\Psi|^2$ represented

as a product of Gaussian functions and the nucleon–nucleon scattering amplitude $f(q)$:

$$\begin{aligned}
 |\Psi(\mathbf{r}_1 \dots \mathbf{r}_A)|^2 &= \prod_{i=1}^A \rho_i(\mathbf{r}_i), \\
 \rho_i &= \exp(-r_i^2/R_A^2), \\
 f(q) &= \frac{i + \alpha}{4\pi} p\sigma \exp\left(-\frac{1}{2} a q^2\right).
 \end{aligned} \quad (8)$$

The R_A^2 values used in the calculations were determined from the relation $R_A^2 = (2/3)(\langle r_A^2 \rangle - \langle r_p^2 \rangle)(1 - A^{-1})^{-1}$ [16] by using the charge radii $\langle r_A^2 \rangle^{1/2}$ of the ${}^3\text{H}$, ${}^3\text{He}$, and ${}^4\text{He}$ nuclei and the proton charge radius $\langle r_p^2 \rangle^{1/2}$, their values being, respectively, 1.76, 1.94, 1.67, and 0.88 fm [17].

The radial wave functions for the allowed ($P_{1/2}$ and $P_{3/2}$) and forbidden ($D_{3/2}^*$, $D_{5/2}^*$, $S_{1/2}^*$, $P_{1/2}^*$, $P_{3/2}^*$, and $S_{1/2}^*$) states were calculated with the same interaction between the clusters as in [5, 7]. In calculating the cross sections in (5) for the fragmentation of ${}^7\text{Li}$ (at a momentum of $P = 3 \text{ GeV}/c$ per nucleon) and ${}^7\text{Be}$ (at a momentum of $P = 1.6 \text{ GeV}/c$ per nucleon) nuclei, the parameters were set to the values of $\sigma = 43 \text{ mb}$, $\alpha = -0.35$, and $a = 0.243 \text{ fm}^{-2}$ for the former and to the values of $\sigma = 42.8 \text{ mb}$, $\alpha = -0.2$, and $a = 0.245 \text{ fm}^{-2}$ for the latter [18].

3. RESULTS AND CONCLUSIONS

Figure 1 shows that our calculations performed for a proton target and for two groups of target nuclei, (C, N, and O) and (Br and Ag), contained in a track emulsion reveal a characteristic dependence of the shape and magnitude of the cross sections on the target mass number—more precisely, on the target radius $R_T \simeq 1.2A^{1/3}$, which determines approximately the width (in the impact parameter b) of the real part of the profile function, $\text{Re}(\omega(b))$, for the cluster–target system. The imaginary parts of this profile function, $\text{Im}(\omega(b))$ (dashed lines), are moderately small and are of secondary importance. For a first approximation, we can assume that this width is close to the sum of the radii of the intranuclear cluster and target nucleus. The results for the (C, N, and O) and (Br and Ag) groups of target nuclei were obtained in [5] by using the averaged profile function of the ${}^3\text{H}$ and ${}^4\text{He}$ nuclei. The proton–target profile functions presented in the lower part of Fig. 1 were calculated with the aid of the two-dimensional Fourier transform of the amplitude, $f_i(q)$ (3), while the corresponding ${}^7\text{Li}$ cross section was calculated according to expression (5). A comparison of the fragmentation cross

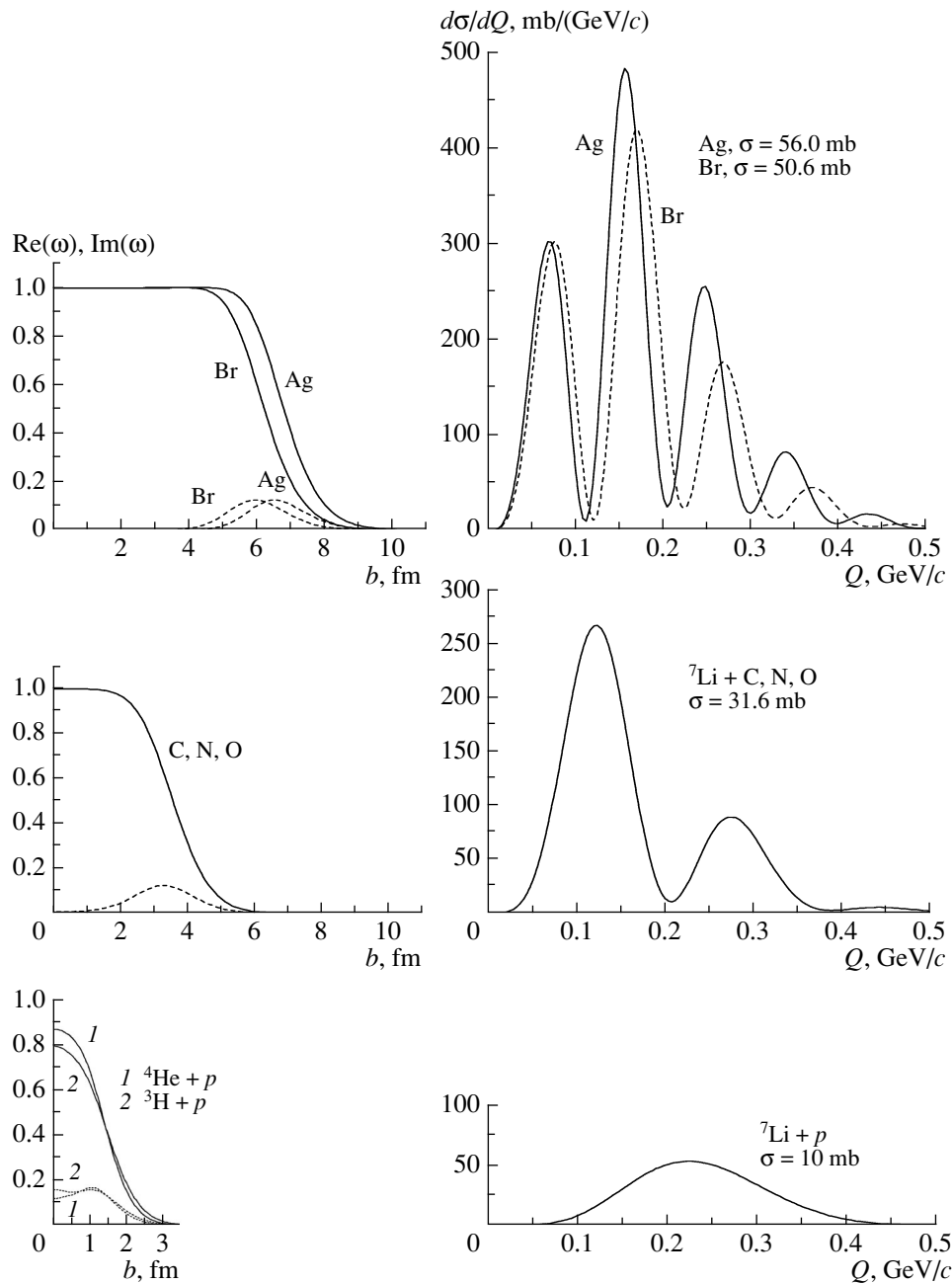


Fig. 1. Profile functions and cross sections for the two-cluster fragmentation of ${}^7\text{Li}$ nuclei (see main body of the text).

sections for heavy and light track-emulsion nuclei and for protons in Fig. 1 shows that, as the target size (profile-function width) decreases, the number of oscillations in the cross sections decreases, while their maxima move toward large values of Q . In the case of a proton target (for pointlike nucleons, $R_T = 0$ and the cross section is determined by the cluster profile function alone), the cross section is characterized by only one maximum greatly shifted to the region around $Q \simeq 0.25 \text{ GeV}/c$ and by a strong

suppression in the regions of $Q \leq 0.1 \text{ GeV}/c$ and $Q \geq 0.35 \text{ GeV}/c$.

In Fig. 2, the cross sections measured by the track-emulsion method for ${}^7\text{Li}$ fragmentation (at a momentum of $P = 3 \text{ GeV}/c$ per nucleon) on nuclei of the (C, N, and O) and (Br and Ag) groups [5] and on protons [13] and the cross section for ${}^7\text{Be}$ fragmentation (at a momentum of $P = 1.6 \text{ GeV}/c$ per nucleon) on protons [14] (histograms in Fig. 2b) are contrasted against the calculated cross sections. The theoretical curve describing the cross sections

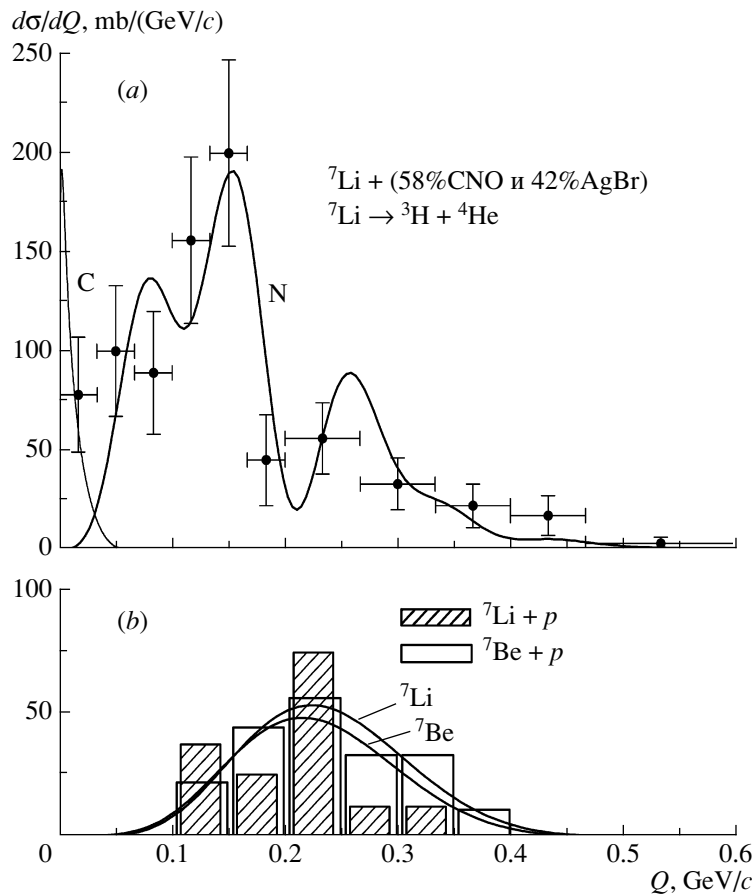


Fig. 2. (a) Experimental data and theoretical curves representing the cross sections for the disintegration of ${}^7\text{Li}$ nuclei on two groups of track-emulsion nuclei, (C, N, and O) and (Br and Ag); (b) experimental data (histograms) and theoretical curves representing the cross sections for the disintegration of ${}^7\text{Li}$ and ${}^7\text{Be}$ nuclei on protons.

for the reactions on complex nuclei (N) was obtained by summing the oscillating diffraction cross sections shown in Fig. 1 [5]. Curve C represents the Coulomb dissociation cross section, which is negligible in the case of proton targets. The smooth curves against the background of the histograms represent the calculated cross sections for the fragmentation of ${}^7\text{Li}$ and ${}^7\text{Be}$ nuclei on a proton target. The difference of these cross sections is moderately small—not more than 15% in the region of the maximum—and one can hardly observe it at the level of a statistical accuracy provided by the track-emulsion method.

We note that, within the two-body model underlying our present calculations and assuming a 100% probability for this type of clustering (the clustering coefficient of $k = 1$), all theoretical cross sections, both for complex target nuclei and for protons, exceed their experimental counterparts. An acceptable description of the absolute values of the cross sections that are shown in Fig. 2 was obtained with a common clustering coefficients of $k = 0.7$. A comparison of the results of our calculations with respective exper-

imental data demonstrates the adequacy of applying the cluster version of Akhiezer–Glauber–Sitenko diffraction theory [8–11] and the two-body cluster model of nuclei that involves forbidden states [6, 7] to describing special features of the experimental cross sections measured for the two-cluster disintegration of relativistic ${}^7\text{Li}$ and ${}^7\text{Be}$ nuclei.

ACKNOWLEDGMENTS

I am grateful to N.G. Peresadko and S.P. Kharlamov for stimulating discussions and enlightening comments on the results of the calculations reported in this article.

This work was supported in part by the Russian Foundation for Basic Research (project no. 12-02-01238-a).

REFERENCES

1. P. I. Zarubin, *Clusters in Nuclei*, Ed. by C. Beck, *Lect. Notes Phys.*: Vol. 875 (Springer, 2013), Vol. 3, p. 51; The BECQUEREL Project. <http://becquerel.jinr.ru/>

2. M. I. Adamovich et al., *Phys. At. Nucl.* **62**, 1378 (1999).
3. M. I. Adamovich, Yu. A. Aleksandrov, S. G. Gerassimov, et al., *J. Phys. G* **30**, 1479 (2004).
4. N. G. Peresadko, Yu. A. Aleksandrov, V. Bradnova, et al., *Phys. At. Nucl.* **70**, 1226 (2007).
5. N. G. Peresadko, V. N. Fetisov, Yu. A. Aleksandrov, et al., *JETP Lett.* **88**, 75 (2008).
6. V. I. Kukulin, V. G. Neudachin, and Yu. F. Smirnov, *Sov. J. Part. Nucl.* **10**, 1006 (1979).
7. S. B. Dubovichenko and M. A. Zhusupov, *Izv. AN KazSSR, Ser. Fiz.-Mat.*, No. 4, 44 (1983).
8. A. I. Akhieser and A. G. Sitenko, *Phys. Rev.* **106**, 1236 (1957).
9. R. Glauber, *Phys. Rev.* **99**, 1515 (1955).
10. M. V. Evlanov, A. M. Sokolov, and V. K. Tartakovsky, *Phys. At. Nucl.* **59**, 647 (1996).
11. V. V. Davidovsky, M. V. Evlanov, and V. K. Tartakovsky, *Phys. At. Nucl.* **69**, 230 (2006).
12. V. N. Fetisov, *Phys. Part. Nucl. Lett.* **11**, 36 (2014).
13. N. G. Peresadko, Yu. A. Aleksandrov, S. G. Gerassimov, et al., *Phys. At. Nucl.* **73**, 1942 (2010).
14. Yu. A. Aleksandrov, N. G. Peresadko, S. G. Gerassimov, et al., *Phys. At. Nucl.* **78**, 363 (2015).
15. W. Czyż and L. Leśniak, *Phys. Lett. B* **24**, 227 (1967).
16. V. Franco and A. Tekou, *Phys. Rev. C* **37**, 1097 (1988).
17. I. Angeli, *At. Data Nucl. Data Tables* **87**, 185 (2004).
18. V. Franco, *Phys. Rev. C* **6**, 748 (1972).